# Neuroimaging for the Nonradiologist

Edward Libfeld, MD
Department of Radiology, Neuroradiology Division, Mount Sinai Beth Israel, New York, New York

Neuroimaging interpretation is truly an art. One of the prerequisites for effective neuroimaging interpretation is a solid understanding of neuroanatomy, which is both complex and intricate. Building upon a foundation of neuroanatomy, a detailed knowledge of pathophysiology is required. One must also have a command of various imaging modalities to correctly apply anatomic and pathophysiological information. This includes an understanding of the physics behind each modality, which will in turn aid in knowing a particular modality's strengths and weaknesses. Blending all of these skills together to make an accurate interpretation while keeping a particular clinical scenario in mind is where the art of neuroimaging is applied. Mastering this process is obviously something that takes years of proper training, meticulous attention to detail, and a background of clinical experience. It is difficult to distill this art form into a small nugget of all-encompassing knowledge; however, a few introductory concepts will go a long way toward improving one's ability to glean useful clinical information from neuroimaging studies.

## Anatomy

Regardless of the modality employed, a solid base of anatomic understanding is critical for correct image interpretation. Modalities may evolve and change, but anatomy is constant. This lends an alternate meaning to Sigmund Freud's saying "Anatomy is destiny."

A neuroimager's arena is the central nervous system (CNS). Information regarding the peripheral nervous system as well as head and neck anatomy is beyond our scope. The CNS consists of the brain and the spinal cord. The following sections describe the most salient CNS neuroanatomy.

Reprints: Edward Libfeld, MD, Department of Radiology, Neuroradiology Division, Mount Sinai Beth Israel, 1st Avenue and 16th Avenue, New York, NY 10003. E-mail: elibfeld@chpnet.org

INTERNATIONAL ANESTHESIOLOGY CLINICS
*Volume 53, Number 1, 123–145*

### Brain

A logical way to describe basic brain anatomy is an outside-to-inside approach.[1] The brain is protected by the skull, which is composed of the frontal bones, parietal bones, temporal bones, and occipital bone. As with many bones, the skull is composed of outer cortex (outer table and inner table) with marrow sandwiched in between. The outer table abuts the soft tissues of the scalp. Along the inner table of the skull is the dura mater, the outermost meningeal membrane. Subjacent to the dura mater is the middle meningeal membrane, the arachnoid mater. The innermost meningeal membrane is the pia mater, which is closely adherent to the outer gyral surfaces of the brain. Although most of the meninges are not well visualized on computed tomography (CT) or magnetic resonance imaging (MRI) in normal healthy patients, there are a few exceptions. Visible infoldings of the dura mater include the falx cerebri and the tentorium cerebelli. The falx cerebri separates the left and right cerebral hemispheres from each other. The tentorium cerebelli, also dura mater infoldings, separate the occipital lobes from the cerebellar hemispheres below. Between the pia mater and the arachnoid mater is the very visible cerebrospinal fluid (CSF) that bathes the brain and spinal cord.

The cerebral hemispheres are composed of the frontal lobes, parietal lobes, temporal lobes, and occipital lobes.[2] It is important to note that sometimes hemispheric lobes are not directly subjacent to bones with the same name. For example, portions of the frontal lobes lie directly under the parietal bones. The central sulcus separates frontal lobes from parietal lobes. The sylvian fissure demarcates frontal and parietal lobes from the temporal lobe below.[3] The occipital lobes are the most dorsal portion of the cerebral hemispheres.

Underlying the outer cortex of the cerebral hemispheric lobes are complex white matter tracts that can most simply be divided into 2 anatomic entities. At the level of the ventricles, the white matter tracts are referred to as the corona radiata. Superior and lateral to the corona radiata, the white matter tracts are collectively known as the centrum semiovale. The corpus callosum is another white matter structure that holds the distinction of being the largest fiber pathway in the brain. Its fibers connect the left and right cerebral hemispheres in a C-shaped configuration flanking the lateral and third ventricles.[4] Going roughly from front to back, the components of the corpus callosum are the rostrum, genu, body, and splenium (Fig. 1). Of note, the anterior and posterior commisures are also white matter tracts that connect the left and right cerebral hemispheres; however, these are much smaller than the corpus callosum. Moving further inferiorly and medially, are white matter tracts known as the internal capsules. The internal capsules

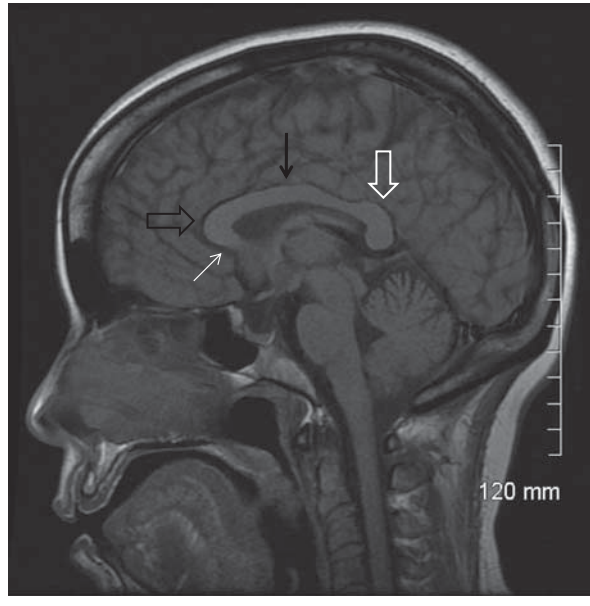


**Figure 1.** *Corpus callosum anatomy, sagittal T1-weighted sequence. Rostrum (white arrow), genu (black open arrow), body (black arrow), and splenium (white open arrow).*

traverse the deep gray matter structures of the brain and are composed of the anterior limb, genu, and posterior limb.[5]

The readily visible deep gray matter structures of the brain include the thalamus, caudate nucleus, globus pallidus, and putamen, which are located in the area between the third ventricle and the sylvian fissures.[6] Flanking the third ventricle are the paired bulbous thalami. The caudate nuclei are C-shaped deep gray matter structures that run along the lateral margins of the lateral ventricles and are separated from the thalami by the genu of the internal capsules. Lateral to the internal capsules is the globus pallidus medially and the putamen laterally. Some common deep gray matter naming conventions in use are important to be aware of. For example, the caudate nucleus, putamen, and globus pallidus are all components of the "basal ganglia" (Fig. 2). Another commonly used term is the "corpus striatum" which includes the caudate nucleus, globus pallidus, putamen, and internal capsule.[7]

Moving further centrally is the ventricular system (Fig. 3). CSF produced within the intraventricular choroid plexus makes its way through the ventricles, bathes the brain and spinal cord, and is in part resorbed into the outer venous sinuses via arachnoid granulations.[8] The paired lateral ventricles are C-shaped structures with multiple components, the largest of which are the lateral ventricular bodies. Anteriorly, the frontal horns of the lateral ventricles are contiguous with the lateral ventricular bodies and abut the caudate nuclei. Posteriorly, the occipital

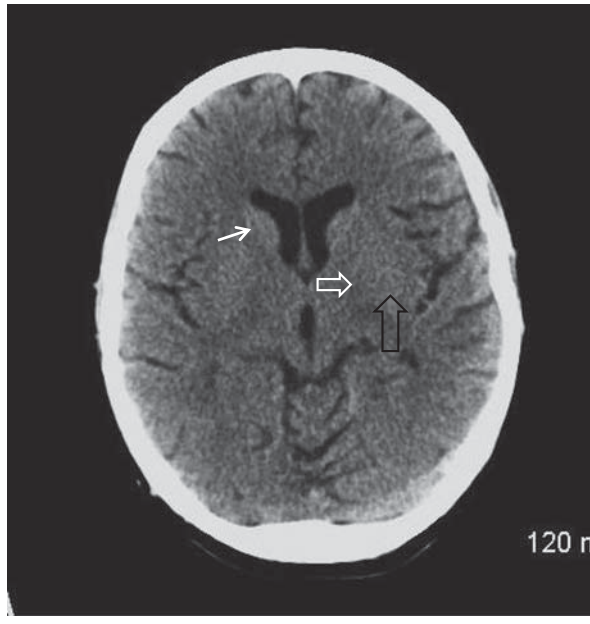


**Figure 2.** *Basal ganglia anatomy, computed tomography. Caudate head (white arrow), globus pallidus (open white arrow), and putamen (open black arrow).*

horns and temporal horns of the lateral ventricles project outward. The temporal horns are closely associated with the hippocampal formations. The temporal horns, occipital horns, and bodies of the lateral ventricles converge upon the trigones of the lateral ventricles (also referred to as the atria of the lateral ventricles). CSF flows from the lateral ventricles into the third ventricle through the Y-shaped foramen of Monro. The third ventricle is a midline structure with multiple recesses flanked by the thalami. From the third ventricle, CSF travels inferiorly into the fourth ventricle through the cerebral aqueduct. The cerebral aqueduct is centrally located within the midbrain just below the tectum. The fourth ventricle is another midline cavity, bounded anteriorly by the pons and flanked by the middle cerebellar peduncles. CSF exits the fourth ventricle inferiorly through the foramen of Magendie at the midline as well as the paired foramina of Luschka laterally.[9]

Paired cranial nerves arise from portions of the brainstem, which is composed of the midbrain, pons, and medulla.[10] The midbrain is the most superior portion of the brainstem and is also referred to as the mesencephalon. Inferior to the midbrain is the pons, and the most caudal portion of the brainstem is the medulla. The tectum of the midbrain, also known as the quadrigeminal plate, is located posterior and superior to the cerebral aqueduct. The cerebral peduncles are

**Figure 3.** *Ventricular system anatomy, T2-weighted sequences. Lateral ventricle body (open arrowhead), lateral ventricle frontal horn (black arrow), foramen of Monro (white arrow), lateral ventricle trigone (open white arrow), third ventricle (white arrowhead), lateral ventricle occipital horn (open black arrow), and fourth ventricle (black arrowhead).*

paired midbrain projections that arise anterolaterally. Surrounding the midbrain are multiple cisterns containing CSF, collectively known as the perimesencephalic cisterns. The interpeduncular cistern is located ventrally between the cerebral peduncles. The quadrigeminal plate cistern is located behind the quadrigeminal plate. The paired ambient cisterns flank the lateral midbrain edges. Immediately ventral to the pons is the prepontine cistern, and lateral to the pons are the cerebellopontine angle cisterns. Immediately ventral to the medulla is the premedullary cistern, and dorsal to the medulla is the cisterna magna at the level of the foramen magnum. Another important cistern worth knowing is the suprasellar cistern. As its name suggests, the suprasellar cistern is located above the sella turcica which houses the pituitary gland.

The cerebellum resides underneath the cerebral hemispheres and behind the brainstem. At the midline is the cerebellar vermis that is in close proximity to the fourth ventricles. The paired cerebellar hemispheres are in contiguity with and flank the cerebellar vermis.[11] The cerebellar hemispheres have a similar internal arrangement to the cerebral hemispheres, with an outer layer of cortex and white matter tracts underneath. As with the cerebral hemispheres, the cerebellar hemispheres contain deep gray matter structures. The largest of these are the paired dentate nuclei that are located near the lateral margins of the fourth ventricle. The cerebellum is connected to the brainstem by the paired cerebellar peduncles. The superior cerebellar peduncles connect to the midbrain, the middle cerebellar peduncles connect to the pons, and the inferior cerebellar peduncles connect to the medulla. The middle cerebellar peduncles are the largest, and each middle cerebellar peduncle is commonly referred to as the brachium pontis.

### *Spine*

The bony elements of the spine protect the spinal cord within. There are 7 cervical vertebrae, 12 thoracic vertebrae, and 5 lumbar vertebrae. The most inferior lumbar vertebral body, L5, articulates with the sacrum which itself has 5 segments. Most spinal vertebrae have a similar configuration: an anterior vertebral body and posterior elements. The posterior elements are comprised of pedicles, articulating facets, laminae, and spinous processes. Thoracic and lumbar vertebrae also have transverse processes, whereas cervical vertebrae do not. The top 2 cervical vertebrae are somewhat unique due to their function in facilitating head motion[12] (Fig. 4). The C2 vertebra, also known as the axis, is the pivot upon which the C1 vertebra, also known as the atlas, rotates. The pivot is the odontoid process, also referred to as the dens, which projects superiorly from the C2 body. The C1 vertebra rotates on the odontoid process.[13] Instead of a body, the C1 vertebra has an

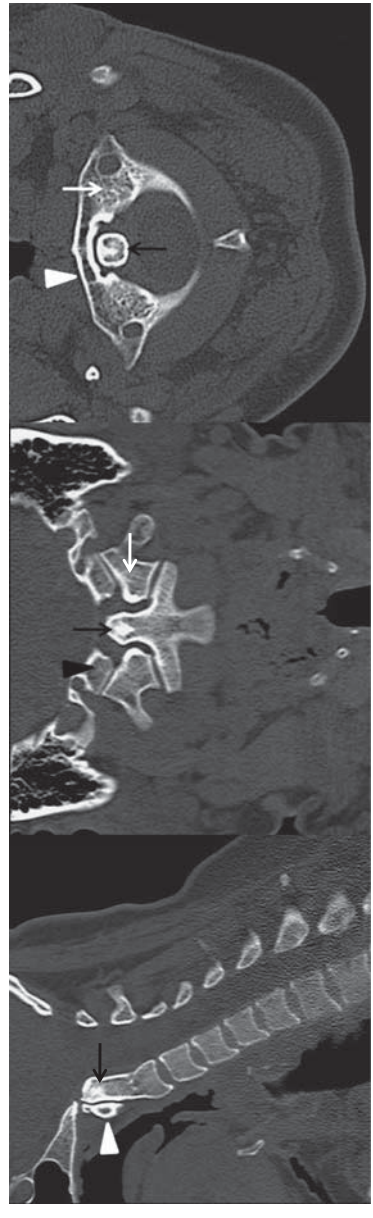

**Figure 4.** *Upper cervical spine anatomy. Sagittal, coronal, axial computed tomography images. Anterior arch of C1 (white arrowhead), odontoid process (black arrow), occipital condyle (black arrowhead), and lateral mass of C1 (white arrow).*

anterior arch and a posterior arch that are connected by lateral masses. Superiorly, the C1 lateral masses articulate with the occipital condyles at the base of the skull.

Much like other bones, the vertebrae have a rigid outer cortex and marrow within. In between the rigid cortical endplates of contiguous vertebral bodies lies the intervertebral disk, which acts as a fibrocartilaginous joint which holds adjoining vertebrae together. The aforementioned articulating facets form facet joints, also called zygapophysial joints, which also serve to hold vertebrae together. The C3-C7 cervical vertebrae also have uncovertebral joints, also known as Luschka's joints, which also connect one vertebra to another.[14] Several spinal ligamentous structures also serve to hold the spine together and allow for spinal mobility. Of note are the anterior and posterior longitudinal ligaments that run along the length of the spine anterior and posterior to the vertebral bodies.

Foraminal openings between spinal elements allow for the passage of neural and vascular structures. The cervical vertebrae contain paired transverse foramina that transmit the cervical vertebral arteries. Typically, the vertebral arteries enter the transverse foramina of the sixth cervical vertebra, skipping the transverse foramina of the seventh vertebra.[15] The paired neural foramina, also known as intervertebral foramina, arise between the pedicles of adjacent vertebral bodies. The neural foramina transmit exiting spinal nerve roots that arise from the spinal cord, as well as segmental spinal arteries and veins.

The inner cavity of the spine is the central canal, also referred to as the spinal canal. Just as with the skull, the central canal is lined by meningeal membranes. The outer rigid dura mater lines the inner surfaces of the central canal, and the middle arachnoid mater is just deep to the dura mater. The pia mater is adherent to the spinal cord. Although the meningeal layers are typically not visible on imaging studies, CSF in between the arachnoid and pial layers is readily apparent. The spinal cord extends inferiorly from the medulla and terminates at approximately the L1 or L2 level. Gray matter is present within the innermost substance of the spinal cord, surrounded by white matter tracts. The spinal cord's most inferior segment is referred to as the conus medullaris. Lumbar spinal nerves emanate inferiorly from the conus medullaris and traverse the CSF within the subarachnoid space. This bundle of spinal nerves is known as the cauda equina.[16]

## ■ Imaging Modalities

### *Radiographs and Fluoroscopy*

Although radiographic examinations are not clinically relevant for imaging the brain or spinal cord they still are useful in several regards,

particularly spinal radiographs. Plain films of the spine can serve as an initial screening test for patients with back pain revealing fractures, vertebral malalignment, and degenerative changes.[17]

Spinal x-rays or flouroscopy performed in the operating room provide surgical localization. A cross-sectional examination (CT or MRI) almost always precedes surgical intervention. Intraoperatively, care must be taken to correlate the level of abnormality found on preoperative examination to the intraoperative localizer plain films. While this may seem straightforward, variations in normal anatomy can make counting vertebral bodies confusing. Transitional lumbosacral segments are relatively common, including sacralization of the L5 vertebra and lumbarization of the S1 vertebra.[18] Therefore, it is critically important that regardless of the enumeration scheme employed, spinal numbering is consistent between all imaging studies. Following surgical intervention, radiographic confirmation of spinal hardware placement is typically performed.[19] Routine spinal radiographic follow-up examinations are performed in postoperative patients to exclude hardware complications such as loosening, infection, hardware fracture, hardware migration, and pseudoarthrosis.

### *Computed Tomography (CT)*

CT is a cross-sectional imaging modality that can be performed quickly, providing detailed anatomic information. Today's multislice CT scanners have the ability to capture imaging data from head to toe within seconds, and are available at all hours. Although the physics behind modern CT is complex, a simple way to understand CT is to compare it to radiography.[20] In radiography, x-ray beams are aimed toward a patient in 1 direction and an image is produced depending on the composition of the tissues with which the x-rays encounter. In CT, the patient moves through a circular rotating gantry, whereas x-rays are directed 360 degrees around the patient's body. This allows for the acquisition of 3-dimensional data which can be reformatted into axial, sagittal, coronal, or oblique planes. The downside of CT is the radiation involved, which becomes an issue when imaging pregnant women and children.[21]

CT can detect 5 basic densities—air, fat, fluid, bone, and metal (Fig. 5). Density in CT images is measured in Hounsfield units (HU). Most of the soft tissues in the human body demonstrate density measurements higher than pure fluid and lower than bone. When describing the appearance of findings on a CT scan, the terms "hypodense" and "hyperdense" are frequently used. Iodinated contrast material can be introduced intravenously to opacify blood vessels and search for abnormal CNS enhancement. CT angiography is accomplished by dynamically scanning while delivering a timed contrast bolus through the blood vessels. CT perfusion data can be obtained by analyzing the degree of brain

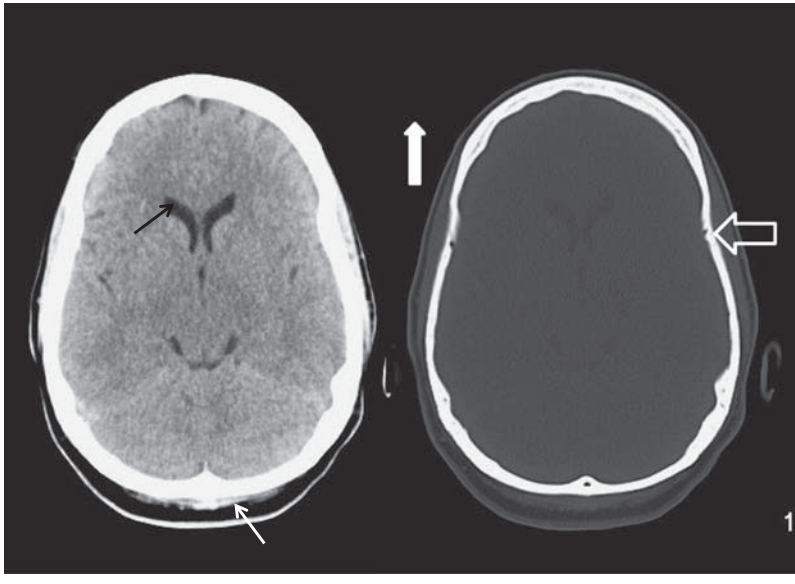

**Figure 5.** *Various computed tomography densities. Cerebrospinal fluid (black arrow), subcutaneous fat (thin white arrow), air (thick white arrow), and bone (open white arrow).*

opacification over time during a dynamic contrast bolus injection.[22] CT myelography is achieved by introducing contrast material into the subarachnoid space of the spine and then scanning.[23] Yet another application of CT is PET/CT.[24] PET/CT fuses the physiological metabolic data of PET imaging to the anatomic detail of CT.

### *Magnetic Resonance Imaging (MRI)*

MRI provides cross-sectional data similar to CT, but with increased soft-tissue detail and contrast. Unlike CT, MRI does not use radiation, making it a preferred modality for imaging pregnant women and children. In simple terms, the hydrogen atoms within the body part of concern are dynamically excited within a strong magnetic field.[25] Following excitation, these hydrogen atoms emit a radiofrequency signal that varies depending on tissue composition. MRI depends on using this signal to construct 3-dimensional data. In comparison with CT, present-day MRI takes longer to perform. As a strong magnetic field is used, patients with contraindicated hardware such as cardiac pacemakers are not able to undergo MRI.[26] In addition, precautions must be taken when working in the highly magnetized MRI suite. Medical equipment used must be MR-approved to avoid patient and caregiver accidents, as well as to diminish the appearance of equipment-related artifacts.[27]

Claustrophobia is another drawback of MRI. Closed scanners require the patient to lie down in a narrow closed tube amid loud noise for a significant amount of time. Open scanners employ shorter tubes and some units allow for the patient to be standing; however, image quality is usually inferior to closed scanners.

MRI parameters can be varied to produce different pulse sequences, each of which has distinct clinical utility. The common pulse sequences in use are T1, T2, T2 FLAIR, diffusion-weighted, susceptibility-weighted, and STIR (Fig. 6). When describing the appearance of findings on an MRI study, the terms "bright" and "hyperintense" are interchangeable, and the terms "dark" and "hypointense" are interchangeable. The terms "hypodense" and "hyperdense" do not apply to MRI. T1-weighted sequences generally follow standard anatomic appearance with bright white matter, darker gray matter, and dark CSF. T2 sequences are the opposite of T1 sequences in the sense that white matter is dark, gray matter is brighter, and CSF is quite bright. In fact, all fluid including edema is bright on T2-weighted imaging. T2 FLAIR sequences are performed through the brain to accentuate this watery brightness. Unlike standard T2-weighted imaging, bright CSF signal is suppressed in T2 FLAIR sequences causing pathologic bright signal to stand out. Diffusion-weighted sequences are critical in diagnosing early infarcts. Diffusion-weighted imaging maps the relative movement of water molecules throughout the brain.[28] Diffusion-weighted imaging tends to be grainy and lacks the soft-tissue detail of other pulse sequences. Apparent diffusion coefficient (ADC) maps are images derived from diffusion-weighted sequence acquisition data that are used together with diffusion-weighted images to diagnose early infarcts. Susceptibility-weighted imaging takes advantage of MRI ferromagnetic properties.[29] Certain stages of blood products and calcific material are ferromagnetic and appear dark on susceptibility-weighted imaging. STIR sequences are commonly employed in spinal imaging as a fat saturation technique. Adipose tissue appears bright on both T1-weighted and T2-weighted imaging, and normal adult vertebrae are filled with bright fatty marrow. Edema related to inflammation or neoplasm also tends to be bright on T2-weighted imaging. A STIR sequence suppresses the bright signal of adipose tissue to highlight the bright signal of degenerative, inflammatory, and neoplastic processes.

The intravascular contrast agent for MRI is a derivative of gadolinium, a rare earth metal. Postcontrast MRI is usually T1 weighted. Contrast material can be bolus injected while scanning dynamically to produce MR perfusion data. One advantage of MRI over CT is the ability to generate high-resolution angiographic images without the need for contrast administration. MR time-of-flight technology is used in this scenario.[30]

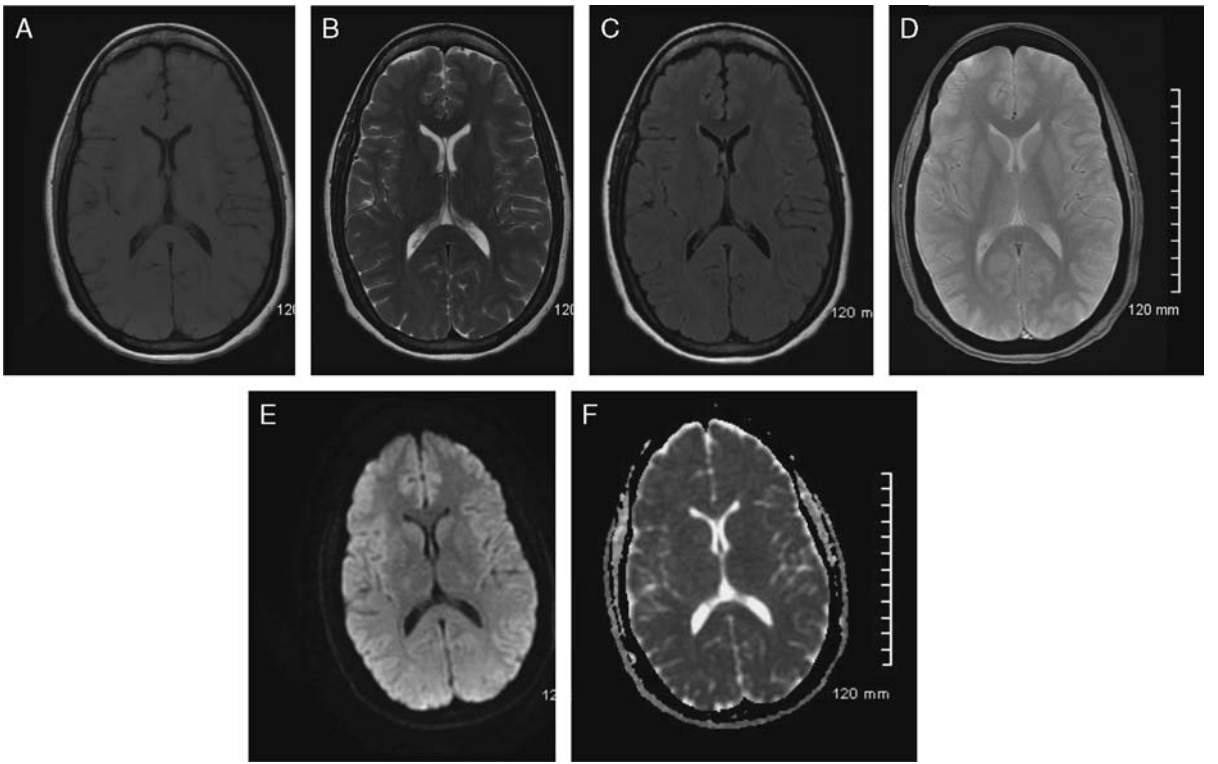


**Figure 6.** *Basic magnetic resonance imaging sequences. T1 (A), T2 (B), T2 FLAIR (C), susceptibility-weighted (D), diffusion-weighted imaging (E), apparent diffusion coefficient map (F).*

### *Angiography*

The gold standard for imaging the neurovasculature has long been catheter angiography.[31] Iodinated contrast material is injected intra-arterially while radiographic imaging is performed in real-time. Contrast runs are captured and can be reexamined to study the arterial, capillary, and venous phases. Advantages of catheter angiography include its 4- dimensional nature, ability to perform interventions, and high resolution. The resolution is such that the tiniest aneurysms and most subtle stenoses can be detected. One of the disadvantages of catheter angiography is its invasive nature and associated risks such as bleeding and stroke.[32] Other disadvantages include expense, time-consuming nature, exposure to radiation, and risks associated with contrast material. Catheter angiography continues to exist as a key imaging and interventional modality; however, it is not considered a first-line screening examination.

## ■ Pathology

The spectrum of CNS pathology is wide. What follows is an overview of common CNS pathologic entities which may be treated surgically and are therefore of importance to an anesthesia caregiver. Disease states including congenital malformations, metabolic aberrations, demyelinating disorders, and several inflammatory entities are beyond our scope.

Surgical decompression is occasionally needed to treat a substantially large space-occupying abnormality because the skull is rigid and does not accommodate increases in intracranial pressure. Once a lesion results in increased intracranial pressure, brain tissue must unfortunately be displaced resulting in brain herniation[33] (Fig. 7). Brain tissue may herniate transversely underneath the falx (subfalcine herniation), above or below the tentorial leaflets (transtentorial herniation), or downward through the foramen magnum (cerebellar tonsillar herniation). Depending on the location of the mass, the medial temporal lobe may herniate toward the midline (uncal herniation).[34] Craniotomy, craniectomy, or cranioplasty may be performed to alleviate these complications.

Frequently, the ventricular system becomes compromised as brain tissue is shifted around. As the choroid plexus within the ventricles constantly produces CSF, pinched-off ventricles will enlarge and will result in further shifting of surrounding brain tissue. When a space-occupying process compromises the ventricular system in this way, it is known as noncommunicating hydrocephalus. When the entire ventricular system enlarges because of a more global disease process (including subarachnoid hemorrhage, meningitis, and venous hypertension), the process is known as communicating hydrocephalus.[35]

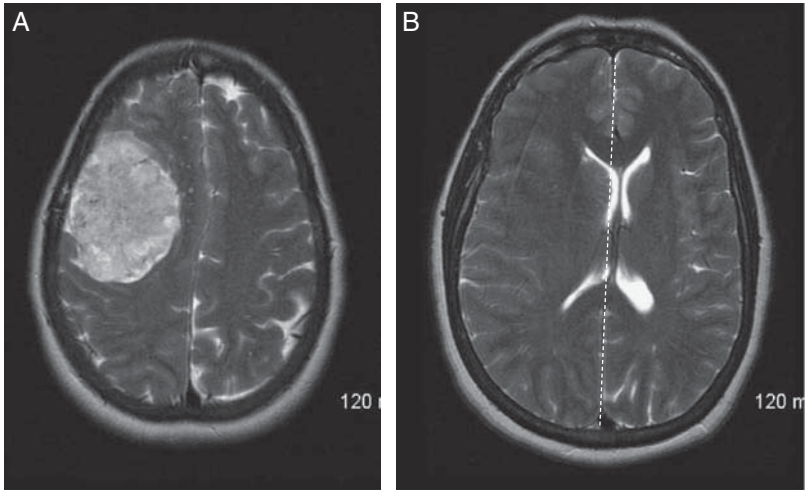


**Figure 7.** *Subfalcine herniation, axial T2-weighted sequences. Large right-sided meningioma (A). Resultant leftward subfalcine herniation. The septum pellucidum is shifted 8 mm leftward from the midline with mild asymmetric distention of the left lateral ventricle (B).*

Ventricular catheters are frequently used to decompress distended ventricles. External ventricular drainage catheters may be placed to temporarily relieve hydrocephalus, whereas ventriculoperitoneal shunt catheters offer more permanent decompression. Shunt system adjustments usually call for follow-up neuroimaging studies to check ventricular caliber.

### Brain

**Hemorrhage** Intracranial hemorrhage may be parenchymal, subarachnoid, subdural, epidural, or intraventricular (Fig. 8). Parenchymal hemorrhage has a myriad of etiologies including hypertension, coagulopathy, infarct, trauma, vascular malformation, neoplasm, and amyloid angiopathy. Parenchymal hemorrhage acts as a space-occupying abnormality causing mass effect and inciting edema.[36] In contrast, subarachnoid hemorrhage typically does not have associated mass effect and instead is in contact with the CSF of sulci and cisterns. Therefore, a lumbar puncture with CSF analysis may be performed to exclude subarachnoid hemorrhage.[37] Although subarachnoid hemorrhage is frequently caused by trauma, aneurysmal bleeding must be ruled out as intracranial aneurysms are treatable and potentially lethal.[38] Subdural hemorrhages are most commonly related to trauma or coagulopathy. In subdural hemorrhages, blood products are interposed within the potential space between the dura mater and arachnoid mater. Adjectives such as "crescent-shaped" are commonly used to describe the

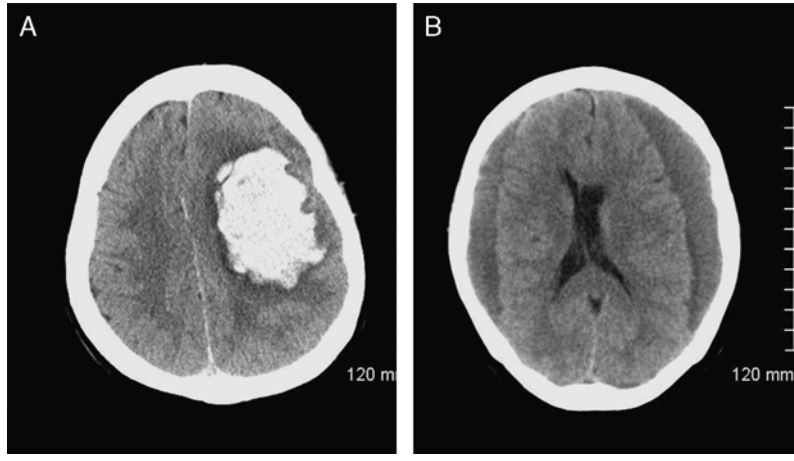


**Figure 8.** *Large acute parenchymal hemorrhage centered at the left frontal centrum semiovale (A). Bilateral subacute subdural hemorrhages, left greater than right. Resultant rightward midline shift (B).*

appearance of subdural hematomas. Epidural hematomas in contrast, are typically described as "biconvex" in morphology. Epidural hematomas are located superficial to the dura mater and underneath the inner table of the skull. Trauma-related arterial injury is usually the culprit for epidural hematomas. As the source of bleeding in epidural hematomas is most commonly arterial, epidural hematomas typically require prompt decompression. It is important to note that all of the aforementioned categories of hemorrhage may also be encountered within the spine, although with much less frequency as compared with intracranial hemorrhage.[39]

As CT is quick and easily accessible, it is usually the first modality used to diagnose hemorrhage. Hyperacute hemorrhage, meaning actively extravasating blood, is somewhat denser than CSF on CT.[40] Acute hemorrhage is more typically encountered and has a hyperdense appearance. As acute blood products evolve into subacute and chronic blood products, they become less and less dense on CT. Subacute blood products may be isodense to brain and therefore difficult to diagnose. Chronic subdural hemorrhages are almost as dense as CSF. Unfortunately, the MR appearance of blood products is not as straightforward.[41] As previously mentioned, certain stages of blood breakdown products appear hypointense on susceptibility-weighted sequences. Also worth noting is that subacute blood products are hyperintense on T1-weighted sequences.

**Infarcts** Cerebral infarcts are typically atherothrombotic or embolic in etiology. Atherothrombotic infarcts commonly occur in arterial vascular territories of the brain, that is, middle cerebral artery territory,

posterior inferior cerebellar artery territory. Therefore, the morphology of atherothrombotic infarcts is dictated by vascular territory. Embolic infarcts have a more varied distribution with involvement of multiple vascular territories. Of note, the term "lacunar infarct" describes a situation where a penetrating artery to the brain's deep structures becomes occluded resulting in infarction.

In the setting of a patient with obvious clinical symptoms related to an acute infarct, a noncontrast CT is useful to rule out associated intracranial hemorrhage that may be a contraindication to certain modes of treatment (ie, TPA). Early signs of infarct on CT are related to infarct edema, such as subtle hypodensity and subtle loss of sulcation[42] (Fig. 9). The natural symmetry of the brain lends itself well toward detecting subtle asymmetric changes. Increased density within an intracranial artery, such as the middle cerebral artery, may be an early sign seen in the setting of infarct. As the infarct evolves into the subacute stage, the infarct becomes more hypodense and associated mass effect progresses. Mass effect secondary to an infarct may necessitate surgical decompression. When the infarct finally evolves into the chronic stage, the result is encephalomalacia, which is essentially nonviable brain tissue. Encephalomalacia is isodense to CSF. In addition to routine noncontrast CT examinations, CT angiography and CT perfusion studies are commonly used in the assessment of infarcts.[43]


**Figure 9.** *Acute left MCA territory infarct on computed tomography. Subtle asymmetric hypodensity and loss of sulcation at the left temporal lobe (black arrowheads). MCA indicates middle cerebral artery.*

One key advantage of MRI in the diagnosis and treatment of infarct is the utilization of the diffusion-weighted sequence.[44] Diffusion-weighted imaging is typically positive immediately at infarct onset, whereas diagnosis on noncontrast CT scan lags behind. Acute and early subacute infarcts demonstrate bright signal on diffusion-weighted sequences with corresponding dark signal on ADC maps (Fig. 10). This combination of bright diffusion signal and corresponding dark ADC signal is known as "restricted diffusion." Tiny recent infarcts may be detected in this manner with MRI, which at the same time would be invisible on conventional noncontrast CT. As an infarct evolves into the late subacute and chronic stages, this diffusion-weighted sequence appearance disappears. Acute and subacute infarcts may demonstrate bright T2 and T2 FLAIR signal. A chronic infarct with resultant encephalomalacia is characterized by signal isointense to CSF, perhaps with a T2 and T2 FLAIR hyperintense rim of gliotic change. MRI of the brain is routinely performed alongside MR angiography and MR perfusion studies in the setting of infarct. Of note, MRI is also useful in diagnosing spinal cord infarcts, which are much more rarely encountered as compared with intracranial infarcts.

**Tumors** Whether in the brain or spinal cord, the first question one must ask when describing a mass is "intra-axial or extra-axial?". Intra-axial means that a lesion is within the substance of the brain and spinal cord itself, and extra-axial encompasses every other localization. Although usually clear-cut, this distinction may at times be rather difficult.[45] Defining a mass as intra-axial or extra-axial opens up 1 set of

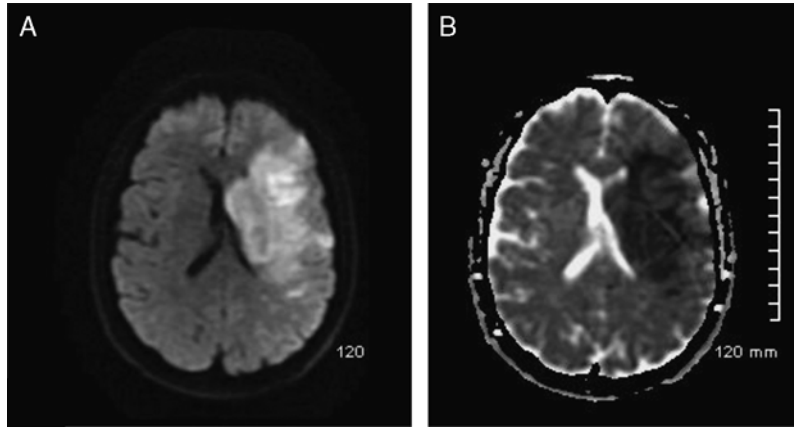


**Figure 10.** *Acute left MCA territory infarct on magnetic resonance imaging, restricted diffusion. Hyperintense signal on diffusion-weighted imaging (A), corresponding hypointense signal on apparent diffusion coefficient map (B). MCA indicates middle cerebral artery.*

differential diagnoses and nullifies a distinct list of diagnostic possibilities. Other features including patient age, clinical history, specific CNS location, morphology, size, and enhancement characteristics are used to further narrow down the differential diagnosis.[46–48]

The most commonly encountered CNS neoplastic lesion is metastatic disease. An enhancing lesion involving the CNS in a patient with a primary malignancy is a metastatic deposit until proven otherwise. Metastatic disease may be either intra-axial or extra-axial and metastasis affects the brain far more frequently than the spinal cord. Metastatic deposits tend to be hypodense on CT and T2/T2 FLAIR hyperintense on MRI; however, appearance varies depending on whether the lesion is hemorrhagic, cystic, or mineralized (Fig. 11). Neoplastic lesions in general tend to incite a larger amount of vasogenic edema as compared with benign entities.

The prototypical example of a high-grade intra-axial primary brain neoplasm is glioblastoma multiforme (GBM). GBM is the most common and most aggressive primary brain malignancy, and unfortunately carries the worst prognosis. Although in some cases GBM may have an appearance identical to a metastatic deposit, GBM tends to be larger, more irregular, and more infiltrative than metastases. On CT, GBM tends to demonstrate irregular thickened margins that may be isodense or hyperdense in comparison with brain tissue. Internal cystic or necrotic change may be present and associated hemorrhage is frequently encountered. GBM is known for inciting a large amount of vasogenic edema and causing profound mass effect. Heterogeneous enhancement is seen on both CT and MRI. The MRI appearance of GBM varies depending on the presence or absence of necrosis, cystic change, and hemorrhage.[49] In general, GBM tends to appear heterogeneously bright on T2 and T2/FLAIR sequences and dark on T1 sequences.

The prototypical and most common extra-axial mass affecting the CNS is the meningioma. Unlike GBM, meningiomas are low-grade tumors and frequently become diagnosed as incidental findings. Meningiomas are most typically encountered intracranially, but a small percentage of meningiomas affect the spine. Most meningiomas appear as spherical extra-axial masses with a broad dural base, but some meningiomas appear as wide curvilinear regions of dural thickening and are referred to as “en plaque” meningiomas. On CT or MRI, meningiomas demonstrate avid enhancement. Meningiomas tend to be hyperdense or isodense to brain tissue or spinal cord on CT and are often times calcified. Reactive calvarial change is sometimes observed on CT, known as hyperostosis. MRI provides more detail in the characterization of meningiomas.[50] Meningiomas tend to be somewhat dark or isointense to adjacent brain tissue on T1 sequences, and demonstrate variable T2 signal. T2 hyperintense edema may be seen in adjacent

**Figure 11.** *Bilateral frontal lobe metastases on magnetic resonance imaging. Axial T1-weighted sequence (A), axial T1 postgadolinium contrast sequence demonstrates lesion enhancement (B), axial T2 FLAIR sequence demonstrates vasogenic edema (C).*

brain tissue or spinal cord. Meningiomas are also known for encasing vascular structures with resultant vessel narrowing.

### Spine

The most commonly diagnosed spinal pathology is chronic degenerative change. Spinal degenerative change is also the most frequent reason for spinal surgery. When characterizing and analyzing spinal degenerative changes it is useful to think in terms of central canal patency and neural foramen patency. As intervertebral disks, ligamentum flavum, uncovertebral joints, and facet joints degenerate they tend to hypertrophy and therefore result in mass effect on adjacent neural elements. Degenerated disks, uncovertebral joints, and facet joints can result in neural foraminal narrowing. Degenerated disks, ligamentum flavum, and facet joints can result in central canal narrowing.

Whether on CT or MRI, normal intervertebral disks demonstrate uniform intact disk height and smooth outer contours that do not extend beyond adjacent vertebral body margins. As a disk degenerates it tends to shrink in craniocaudal dimension and there may be associated discogenic changes in the adjacent endplates. On MRI, normal intervertebral disks demonstrate internal bright T2 signal indicative of disk hydration. Degenerated disks become dessicated and dark on T2-weighted sequences. A diffuse disk bulge is commonly observed which can cause narrowing of both the central canal and the neural foramina. A more focal disk herniation may be superimposed upon a disk bulge and may occur independent of a disk bulge. Disk herniations are in part

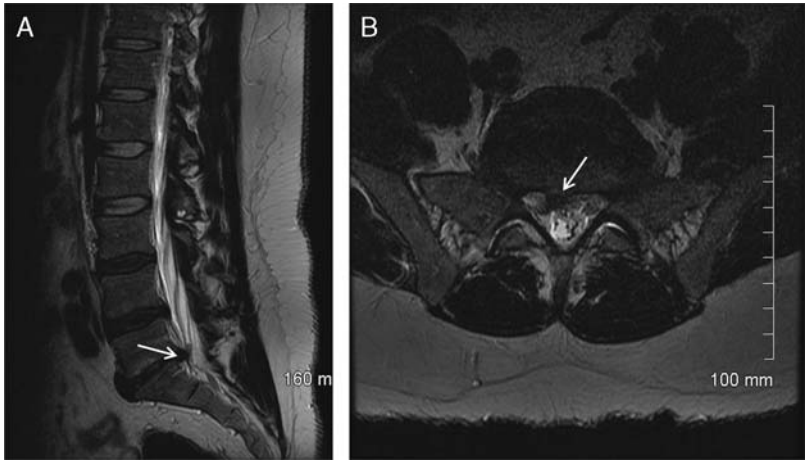


**Figure 12.** *Right paracentral disc herniation at L5-S1 (white arrow) abuts the adjacent traversing right S1 nerve root. Sagittal T2-weighted sequence (A), axial T2-weighted sequence (B).*

characterized by their location along the outer disk margin.[51] A disk herniation may be central, paracentral, foraminal, or extraforaminal. A disk herniation's location, size, and morphology determine whether there may be resultant compression of neural elements in the central canal, neural foramen, or both (Fig. 12).

## ■ Conclusions

In today's interdisciplinary team-oriented approach to patient care it is important for health care providers to all speak the same language. Therefore, a basic understanding of neuroimaging is essential to all clinicians involved in the treatment of CNS disorders, including anesthesiologists. CNS pathology tends to require complex treatment solutions, necessitating a strong background understanding of neuroimaging. Although mastery of neuroimaging takes years of training and experience, a little bit of knowledge can go a long way.

The author declares that there is nothing to disclose.

## ■ References

1. Snell R. *Clinical Neuroanatomy*. Philadelphia: Lippincott Williams & Wilkins; 2010.
2. Ribas GC. The cerebral sulci and gyri. *Neurosurg Focus*. 2010;2:E2.
3. Collice M, Collice R, Riva A. Who discovered the sylvian fissure? *Neurosurgery*. 2008;4:623–628.
4. Battal B, Kocaoglu M, Akgun V, et al. Corpus callosum: normal imaging appearance, variants and pathologic conditions. *J Med Imaging Radiat Oncol*. 2010;6:541–549.
5. Manelfe C, Clanet M, Gigaud M, et al. Internal capsule: normal anatomy and ischemic changes demonstrated by computed tomography. *Am J Neuroradiol*. 1981;2:149–155.
6. Herrero MT, Barcia C, Navarro JM. Functional anatomy of thalamus and basal ganglia. *Childs Nerv Syst*. 2002;8:386–404.
7. Rolls ET. Neurophysiology and cognitive functions of the striatum. *Rev Neurol*. 1994;8:648–660.
8. Kapoor KG, Katz SE, Grzybowski DM, et al. Cerebrospinal fluid outflow: an evolving perspective. *Brain Res Bul*. 2008;6:327–334.
9. Sharifi M, Ungier E, Ciszek B, et al. Microsurgical anatomy of the foramen of Luschka in the cerebellopontine angle, and its vascular supply. *Surg Radiol Anat*. 2009;6: 431–437.
10. Casselman J, Mermuys K, Delanote J, et al. MRI of the cranial nerves—more than meets the eye: technical considerations and advanced anatomy. *Neuroimaging Clin N Am*. 2008;2:197–231.
11. Monte Bispo RF, Casado Ramalho AJ, Buarque de Gusmão LC, et al. Cerebellar vermis: topography and variations. *Int J Morphol*. 2010;28:439–443.
12. Iannacone WM, DeLong WG, Born CT, et al. Dynamic computerized tomography of the occiput-atlas-axis complex in trauma patients with odontoid lateral mass asymmetry. *J Trauma*. 1990;30:1501–1505.

13. Pang D, Li V. Atlantoaxial rotatory fixation: part 1—biomechanics of normal rotation at the atlantoaxial joint in children. *Neurosurgery*. 2004;55:614–625.
14. Hartman J. Anatomy and clinical significance of the uncinate process and uncovertebral joint: a comprehensive review. *Clin Anat*. 2014;27:431–440.
15. Uchino A, Saito N, Takahashi M, et al. Variations in the origin of the vertebral artery and its level of entry into the transverse foramen diagnosed by CT angiography. *Neuroradiology*. 2013;55:585–594.
16. Cohen MS, Wall EJ, Kerber CW, et al. The anatomy of the cauda equina on CT scans and MRI. *J Bone Joint Surg Br*. 1991;73:381–384.
17. Duane TM, Dechert T, Brown H, et al. Is the lateral cervical spine plain film obsolete? *J Surg Res*. 2008;147:267–269.
18. Konin GP, Walz DM. Lumbosacral transitional vertebrae: classification, imaging findings, and clinical relevance. *AJNR Am J Neuroradiol*. 2010;31: 1778–1786.
19. Molinari RW, Hunter JG, McAssey RW. In-hospital postoperative radiographs for instrumented single-level degenerative spinal fusions: utility after intraoperative fluoroscopy. *Spine J*. 2012;12:559–567.
20. Goldman LW. Principles of CT and CT technology. *J Nucl Med Technol*. 2007;35: 115–128.
21. Smith-Bindman R, Lipson J, Marcus R, et al. Radiation dose associated with common computed tomography examinations and the associated lifetime attributable risk of cancer. *Arch Intern Med*. 2009;169:2078–2086.
22. Hoeffner E, Case I, Jain R, et al. Cerebral perfusion CT: technique and clinical applications. *Radiology*. 2004;231:632–644.
23. Hoeffner EG, Mukherji SK, Srinivasan A, et al. Neuroradiology back to the future: spine imaging. *AJNR Am J Neuroradiol*. 2012;33:999–1006.
24. Schöder H, Erdi YE, Larson SM, et al. PET/CT: a new imaging technology in nuclear medicine. *Eur J Nucl Med Mol Imaging*. 2003;30:1419–1437.
25. Plewes DB I, Kucharczyk W. Physics of MRI: a primer. *J Magn Reson Imaging*. 2012;35:1038–1054.
26. Hand PJ, Wardlaw JM, Rowat AM, et al. Magnetic resonance brain imaging in patients with acute stroke: feasibility and patient related difficulties. *J Neurol Neurosurg Psychiatry*. 2005;76:1525–1527.
27. Kanal E, Borgstede JP, Barkovich AJ, et al. American College of Radiology white paper on MR safety. *AJR Am J Roentgenol*. 2002;178:1335–1347.
28. Crawley AP, Poublanc J, Ferrari P, et al. Basics of diffusion and perfusion MRI. *Appl Radiol*. 2003;32:13–24.
29. Robinson RJ, Bhuta S. Susceptibility-weighted imaging of the brain: current utility and potential applications. *J Neuroimaging*. 2011;21:189–204.
30. Heiserman JE, Drayer BP, Fram EK, et al. Carotid artery stenosis: clinical efficacy of two-dimensional time-of-flight MR angiography. *Radiology*. 1992;182:761–768.
31. Zhang WW, Harris LM, Dryjski ML. Should conventional angiography be the gold standard for carotid stenosis? *J Endovasc Ther*. 2006;13:723–728.
32. Leffers AM, Wagner A. Neurologic complications of cerebral angiography. A retrospective study of complication rate and patient risk factors. *Acta Radiol*. 2000;41:204–210.
33. Mokri B. The Monro-Kellie hypothesis applications in CSF volume depletion. *Neurology*. 2001;56:1746–1748.
34. Johnson PL, Eckard DA, Chason DP, et al. Imaging of acquired cerebral herniations. *Neuroimaging Clin N Am*. 2002;12:217–228.
35. Orešković D, Klarica M. Development of hydrocephalus and classical hypothesis of cerebrospinal fluid hydrodynamics: facts and illusions. *Prog Neurobiol*. 2011;94: 238–258.

36. Balami JS, Buchan AM. Complications of intracerebral haemorrhage. *Lancet Neurol*. 2012;11:101–118.
37. Sidman R, Connolly E, Lemke T. Subarachnoid hemorrhage diagnosis: lumbar puncture is still needed when the computed tomography scan is normal. *Acad Emerg Med*. 1996;3:827–831.
38. Mayberg MR, Batjer HH, Dacey R, et al. Guidelines for the management of aneurysmal subarachnoid hemorrhage: a statement for healthcare professionals from a special writing group of the Stroke Council, American Heart Association. *Stroke*. 1994;25:2315–2328.
39. Braun P, Kazmi K, Nogués-Meléndez P, et al. MRI findings in spinal subdural and epidural hematomas. *Eur J Radiol*. 2007;64:119–125.
40. Greenberg J, Cohen WA, Cooper PR. The "hyperacute" extraaxial intracranial hematoma: computed tomographic findings and clinical significance. *Neurosurgery*. 1985;17:48–56.
41. Bradley WG. MR appearance of hemorrhage in the brain. *Radiology*. 1993;189:15–26.
42. de Lucas EM, Sánchez E, Gutiérrez A, et al. CT protocol for acute stroke: tips and tricks for general radiologists. *Radiographics*. 2008;28:1673–1687.
43. Srinivasan A, Goyal M, Al Azri F, et al. State-of-the-art imaging of acute stroke. *Radiographics*. 2006;26:S75–S95.
44. Powers WJ. Testing a test: a report card for DWI in acute stroke. *Neurology*. 2000;54:1549–1551.
45. George AE, Russell EJ, Kricheff II. White matter buckling: CT sign of extraaxial intracranial mass. *AJR Am J Roentgenol*. 1980;135:1031–1036.
46. Al-Okaili RN, Krejza J, Woo J, et al. Intraaxial brain masses: MR imaging-based diagnostic strategy—initial experience. *Radiology*. 2007;243:539–550.
47. Essiga M, Anzaloneb N, Combsc SE, et al. MR imaging of neoplastic central nervous system lesions: review and recommendations for current practice. *AJNR Am J Neuroradiol*. 2012;33:803–817.
48. Al-Okaili RN, Krejza J, Wang S, et al. Advanced MR imaging techniques in the diagnosis of intraaxial brain tumors in adults. *Radiographics*. 2006;26:S173–S189.
49. Bohman LE, Swanson KR, Moore JL, et al. Magnetic resonance imaging characteristics of glioblastoma multiforme: implications for understanding glioma ontogeny. *Neurosurgery*. 2010;67:1319–1327.
50. Carpeggiani P, Crisi G, Trevisan C. MRI of intracranial meningiomas: correlations with histology and physical consistency. *Neuroradiology*. 1993;35:532–536.
51. Fardon DF, Milette PCCombined Task Forces of the North American Spine Society, American Society of Spine Radiology, and American Society of Neuroradiology. Nomenclature and classification of lumbar disc pathology. Recommendations of the Combined Task Forces of the North American Spine Society, American Society of Spine Radiology, and American Society of Neuroradiology. *Spine*. 2001;26:E93–E113.